Multiantenna GPR data acquisition design

Raul Cova*, Matthew Yedlin[1], Dave Henley, Jean-Yves Dauvignac[2], Nicolas Fortino[2], Kevin Hall, Christian Pichot[3] and Stéphane Gaffet[3]

[1]Department of Electrical and Computer Engineering
University of British Columbia

[2]Laboratoire d'Electronique, Antennes et Télécommunications (LEAT)
Université Nice-Sophia Antipolis

[3]Low Background Noise Inter-disciplinary Underground Science and Technology
LSBB Underground Research Laboratory

Agenda

- Introduction
  - MIGA Project
  - LSBB Site
- Electromagnetic vs seismic waves
- Acquisition modelling
- Conclusions
- Acknowledgements

Matter wave - laser based Interferometer Gravitation Antenna (MIGA) project

- “The applications of MIGA extend from monitoring the evolution of the gravitational field to providing a new tool for detecting gravitational waves” (Bouyer, 2011).

MIGA ≠ LIGO (Laser Interferometer Gravitational-wave Observatory)

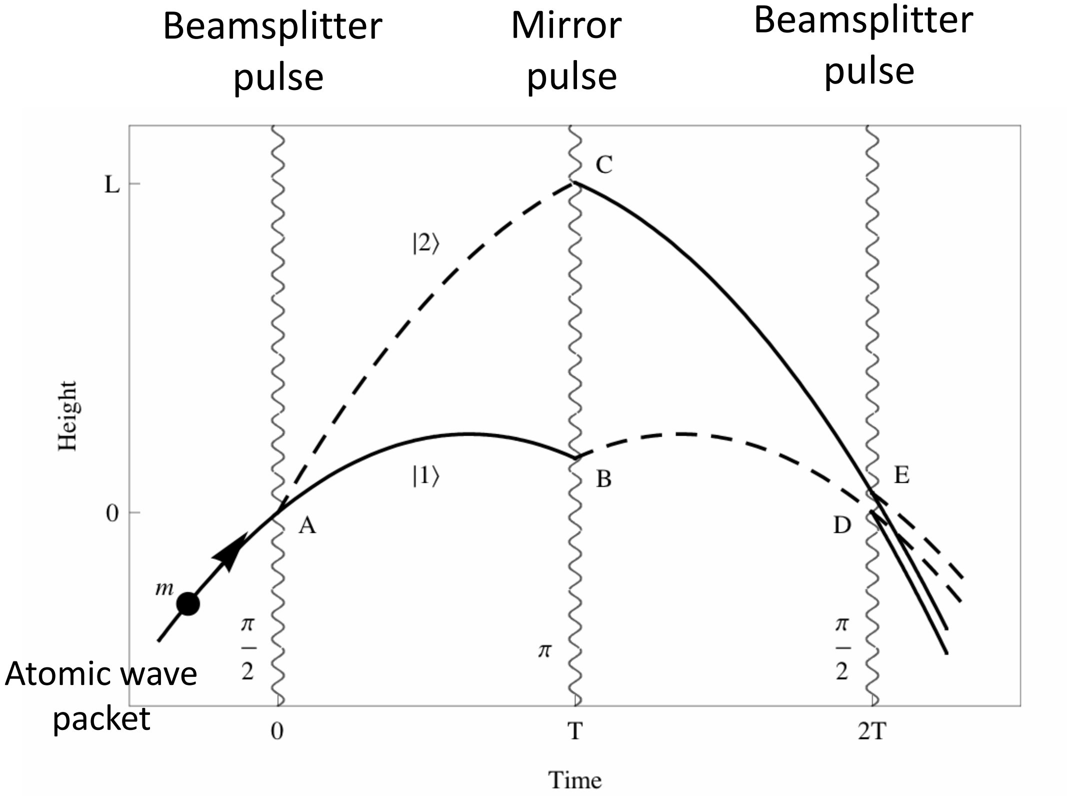

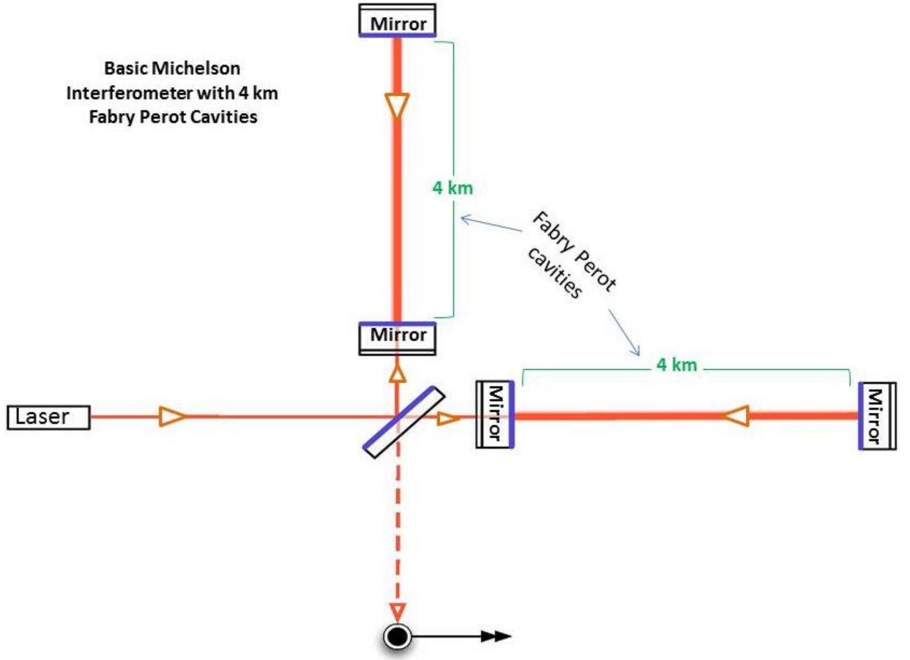

http://scienceblogs.com/principles/2013/10/22/quantum-erasure/

LSBB (Laboratoire Souterrain à Bas Bruit, Rustrel, France)

Goal: to monitor water saturated sediments beneath the LSBB tunnel

maps.google.com

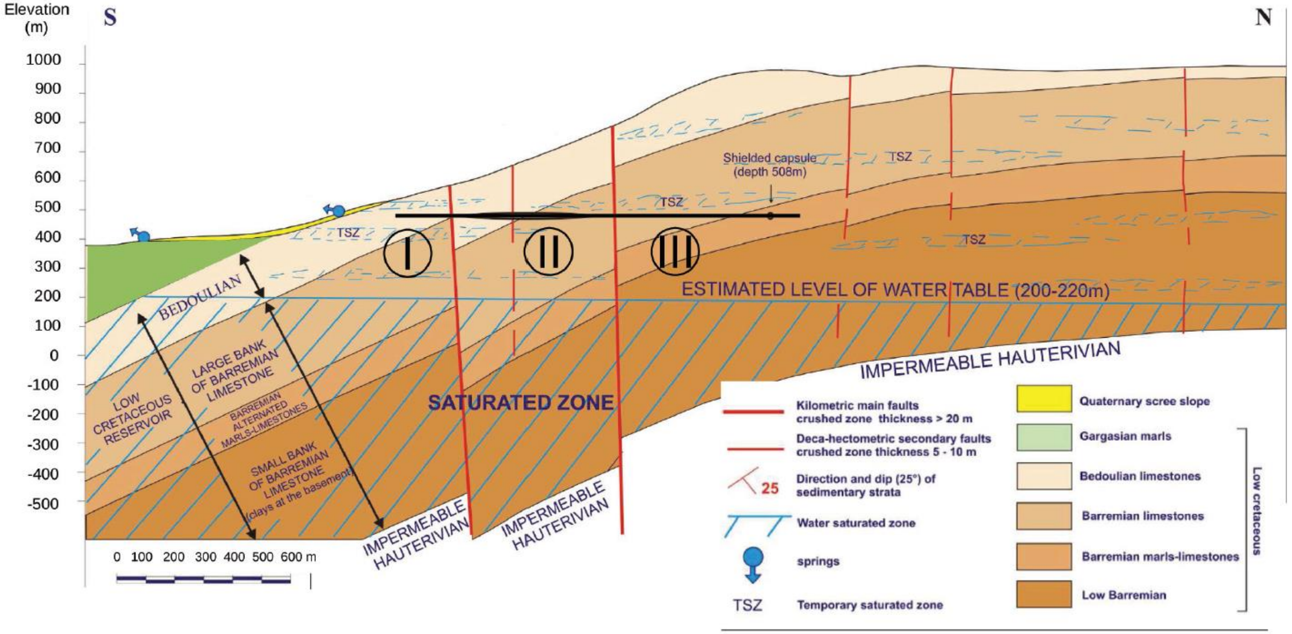

From Senechal (2013)

Seismic and electromagnetic waves

- Despite having different polarizations, TE mode electromagnetic waves can be modelled as an acoustic wave (Laurain and Lecomte, 2001)

$$\nabla^2\Phi - \frac{1}{v^2}\frac{\partial\Phi}{\partial t^2} = 0$$

$$\nabla^2 E - \mu\epsilon\frac{\partial E}{\partial t^2} = 0$$

μ = magnetic permeability
ϵ = dielectric permittivity

$$Z = \rho v$$

$$\rho \rightarrow \mu$$

$$v \rightarrow \frac{1}{\sqrt{\mu\epsilon}}$$

$$Z \rightarrow \mu\frac{1}{\sqrt{\mu\epsilon}} = \sqrt{\frac{\mu}{\epsilon}} = \eta$$

η = Electromagnetic impedance

Acoustic wave reflection coefficient

$$R_{AW} = \frac{Z_2\cos\theta_i - Z_1\cos\theta_t}{Z_2\cos\theta_i + Z_1\cos\theta_t}$$

TE mode reflection coefficient

$$R_{TE} = \frac{\eta_2\cos\theta_i - \eta_1\cos\theta_t}{\eta_2\cos\theta_i + \eta_1\cos\theta_t}$$

Antenna Array

Operation frequencies: 100MHz – 1.5GHz

Assuming v=10cm/ns, $\lambda/4$ = 0.1m @ 250MHz

Original Design: Max Offset 3.8m

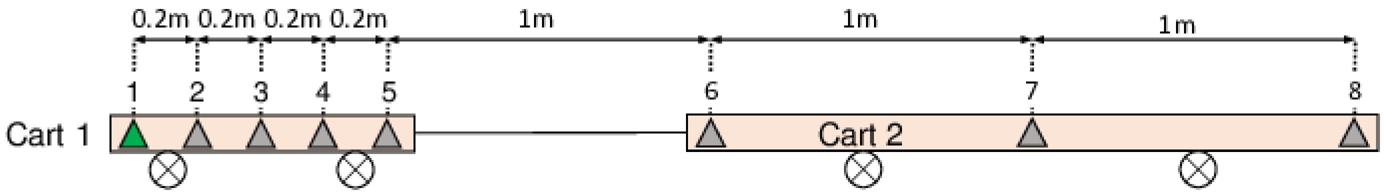

Extended Design:
Max Offset 6.8m

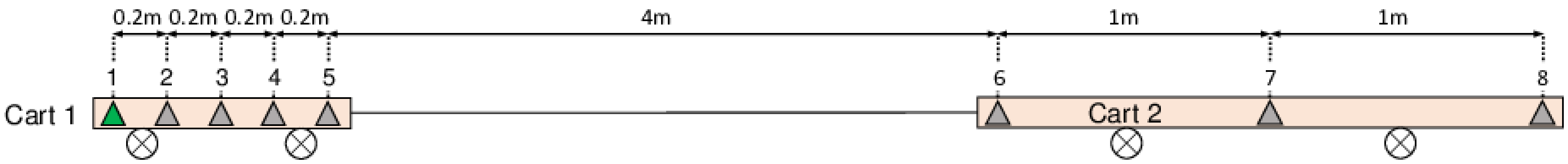

Acquisition sequence

- The first antenna in the array sends a signal which is recorded by all the other antennas and itself
- At each antenna array position eight “source” gathers are recorded, each one of them consisting of eight radargrams
- The antenna array is displaced 10cm and each antenna is fired again.

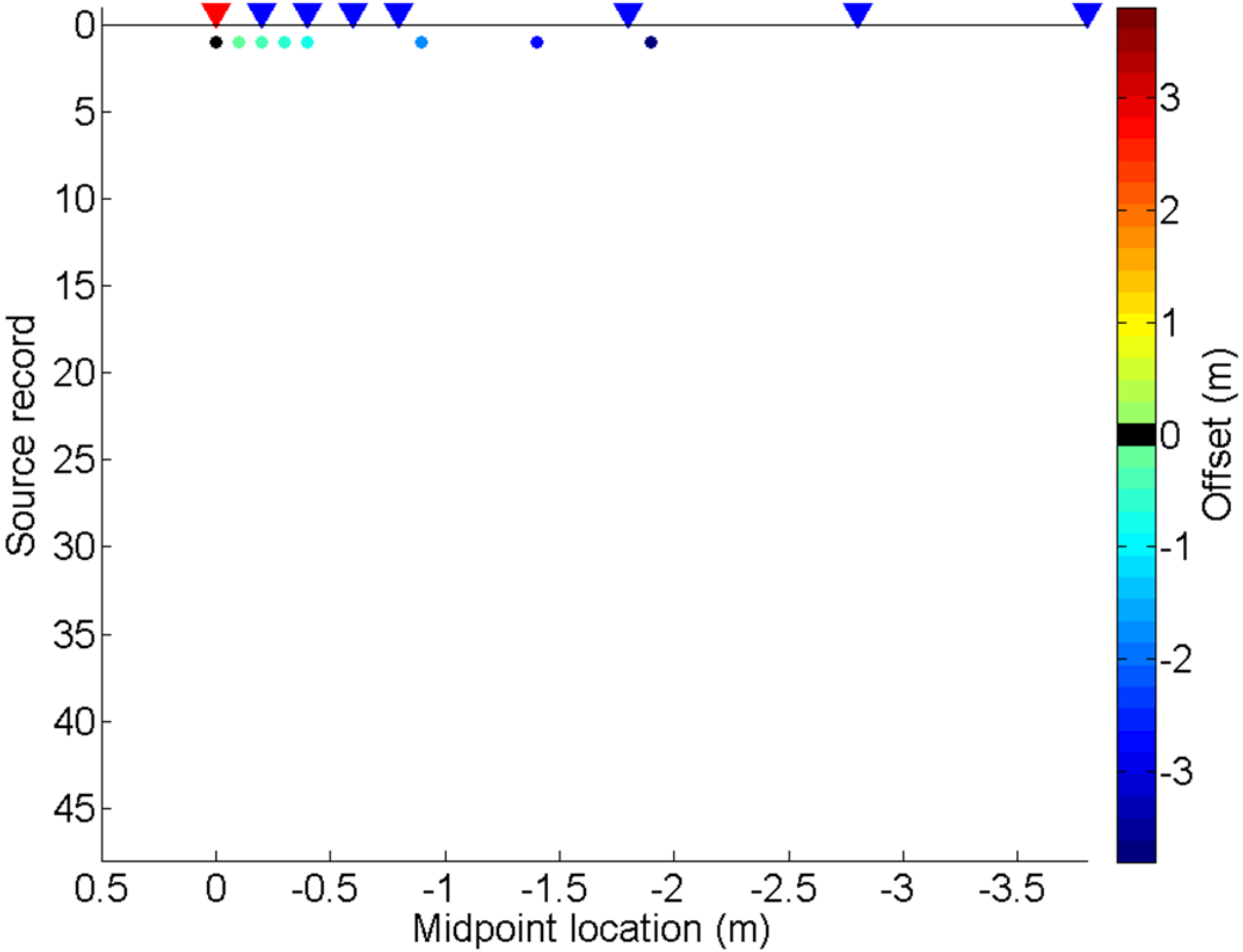

Acquisition sequence

- The first antenna in the array sends a signal which is recorded by all the other antennas and itself
- At each antenna array position eight "source" gathers are recorded, each one of them consisting of eight radargrams
- The antenna array is displaced 10cm and each antenna is fired again.

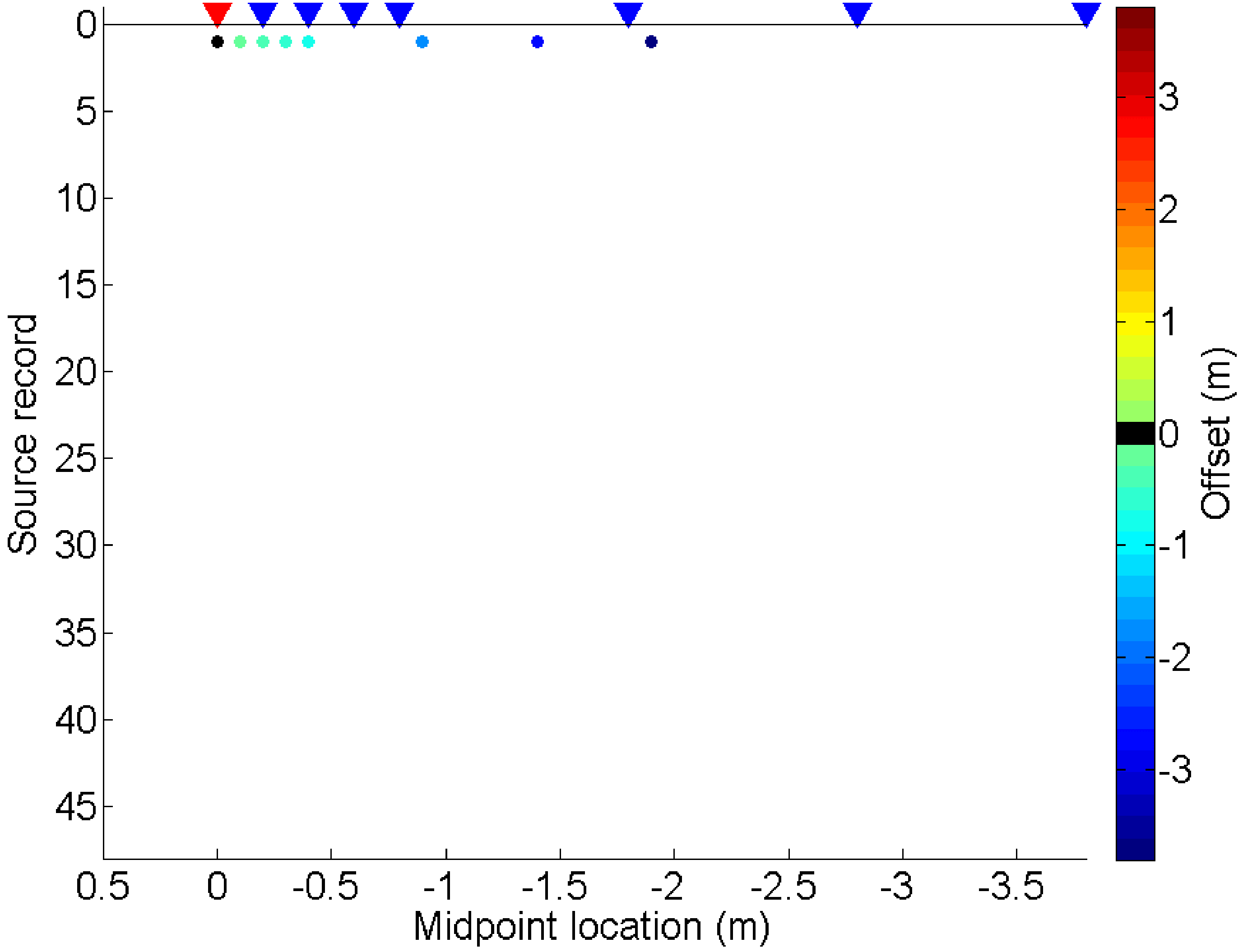

Offsets redundancy

- Midpoints will be sampled several times with the same source-receiver distance, but using different source-receiver pairs.

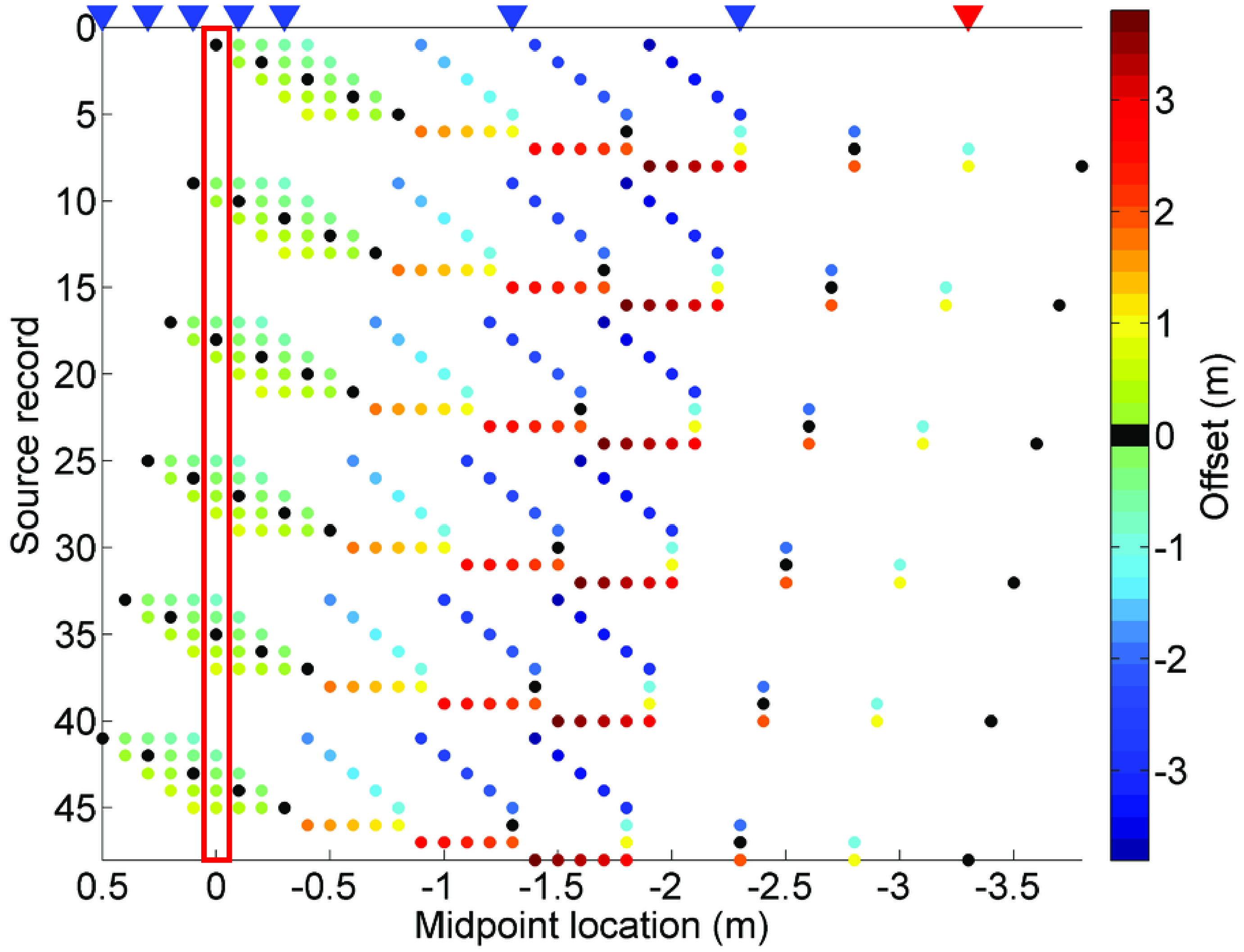

Fold profile and offset distribution: Original setup

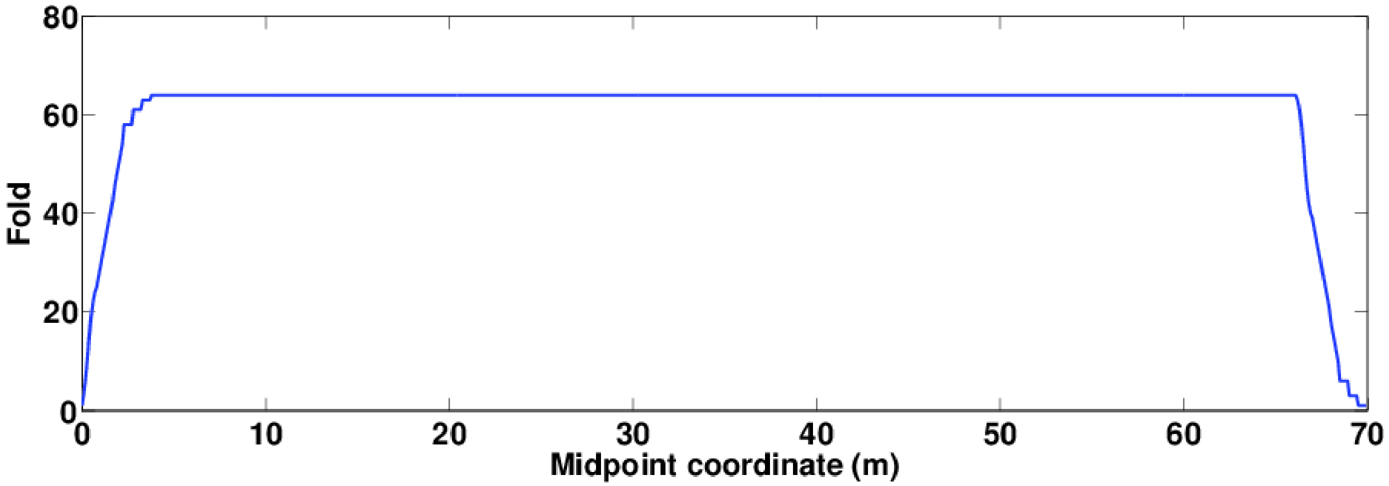

- 64 radargrams per CMP

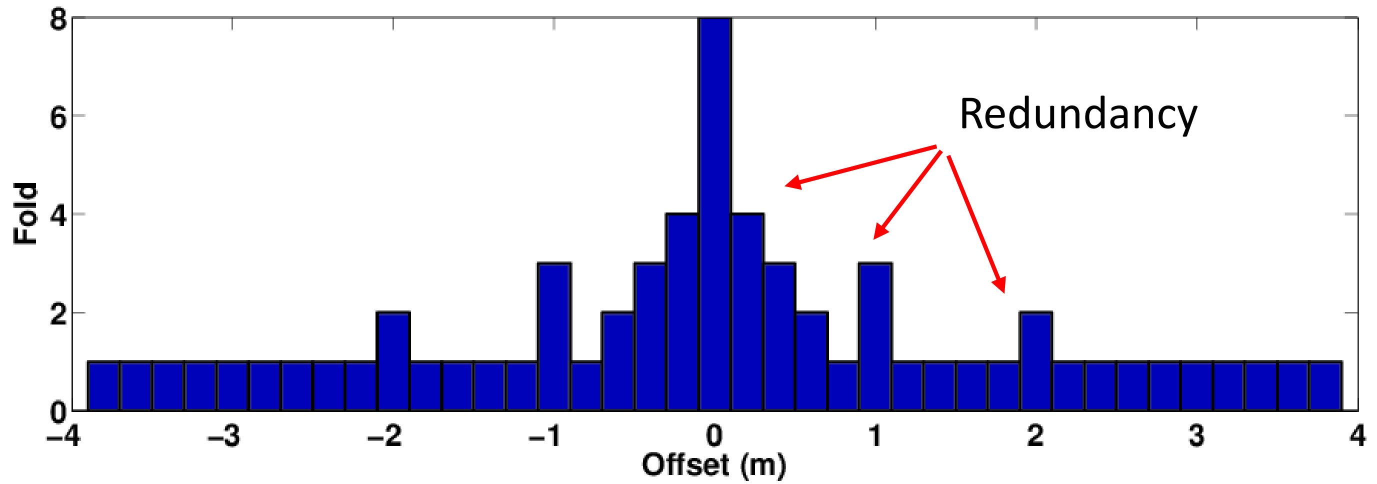

- 39 unique offsets, uniformly sampled (0.2m)

Fold profile and offset distribution: Extended setup

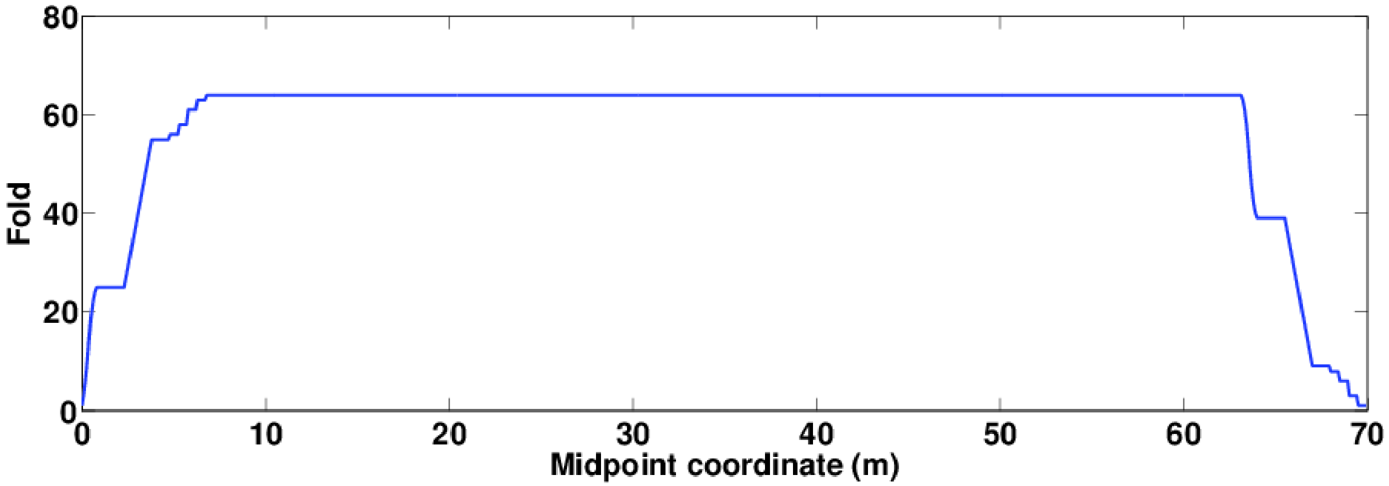

- Fold taper length increased

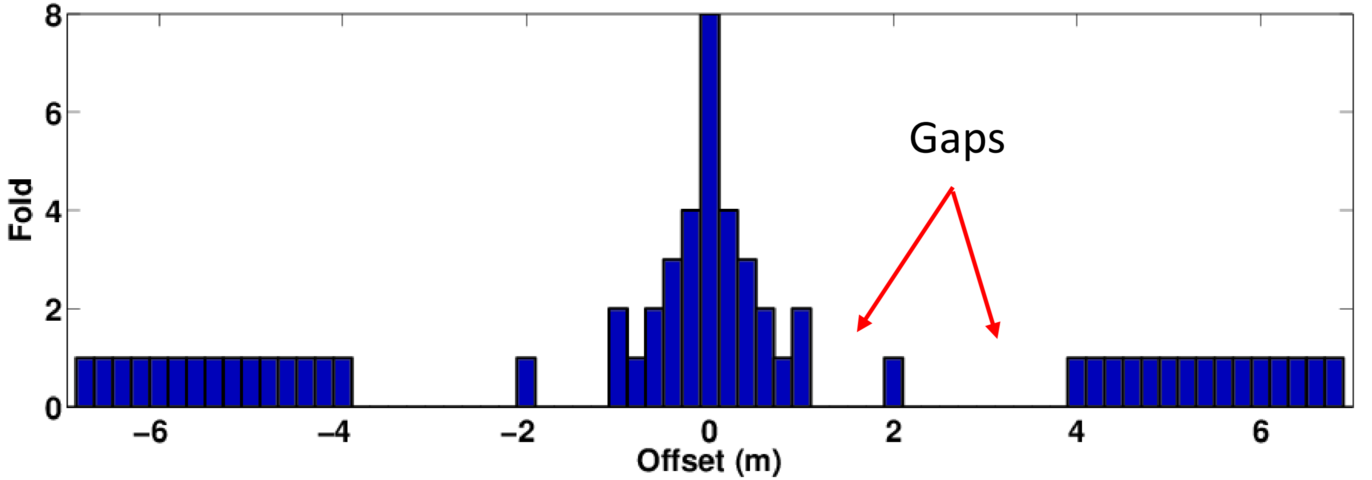

- Irregular offset sampling

Velocity model building

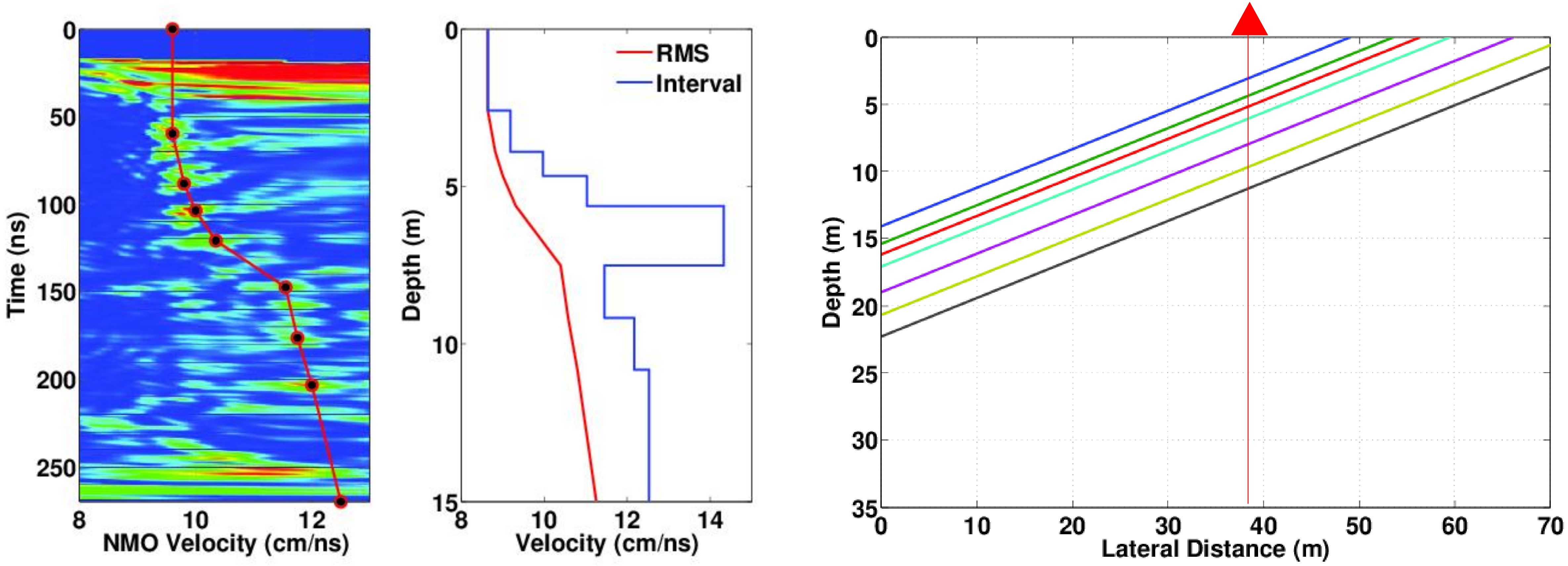

Semblance spectrum from Senechal (2013)

CMP data and velocity analysis: original setup

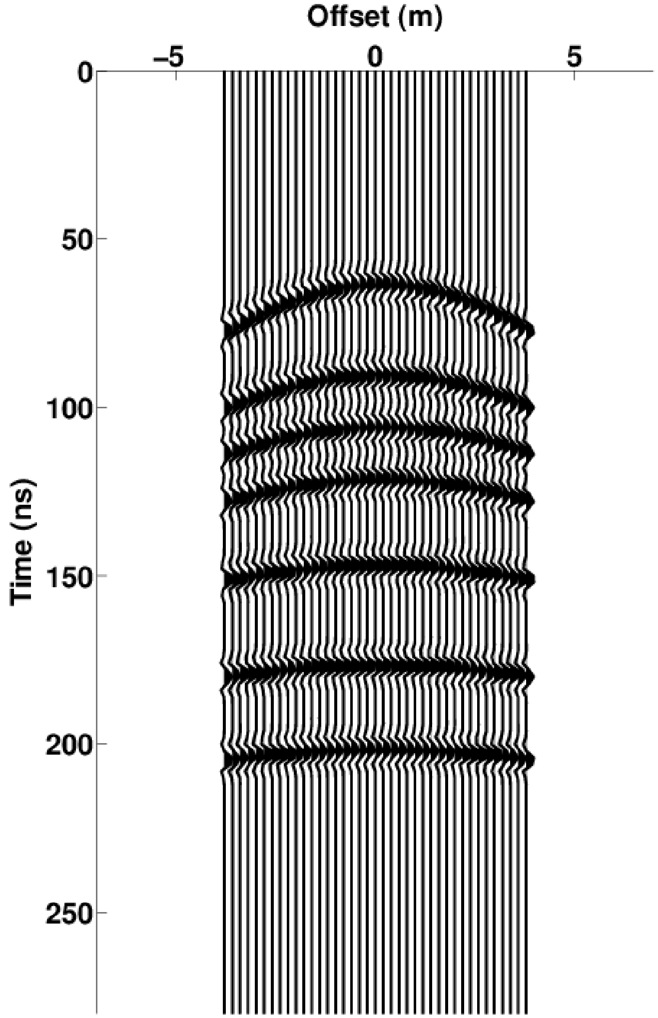

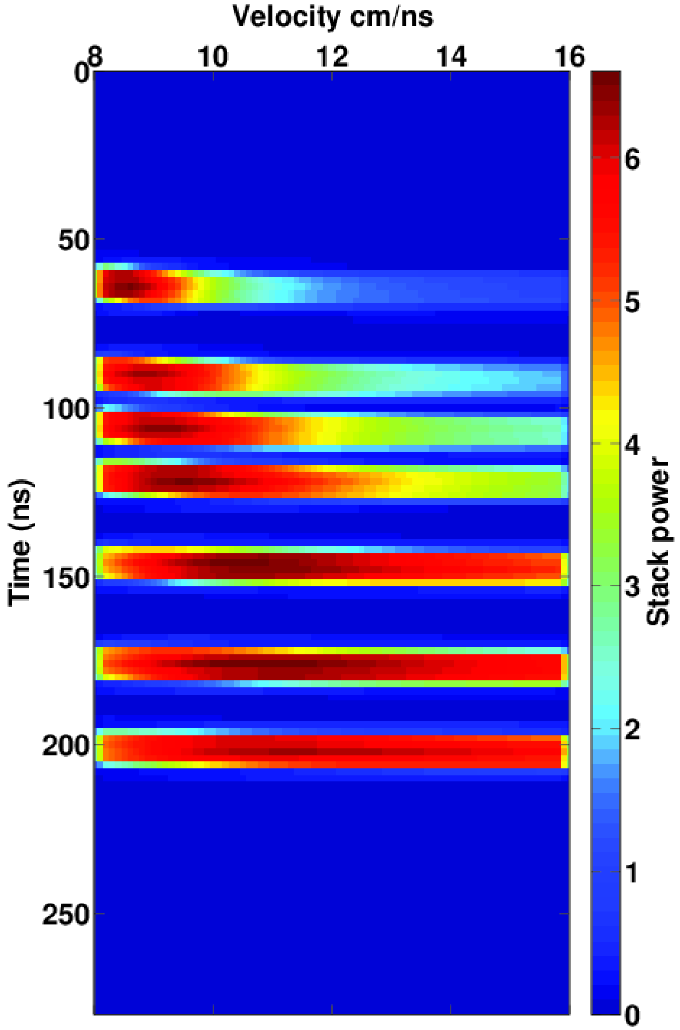

- Poor velocity resolution

CMP data and velocity analysis: extended setup

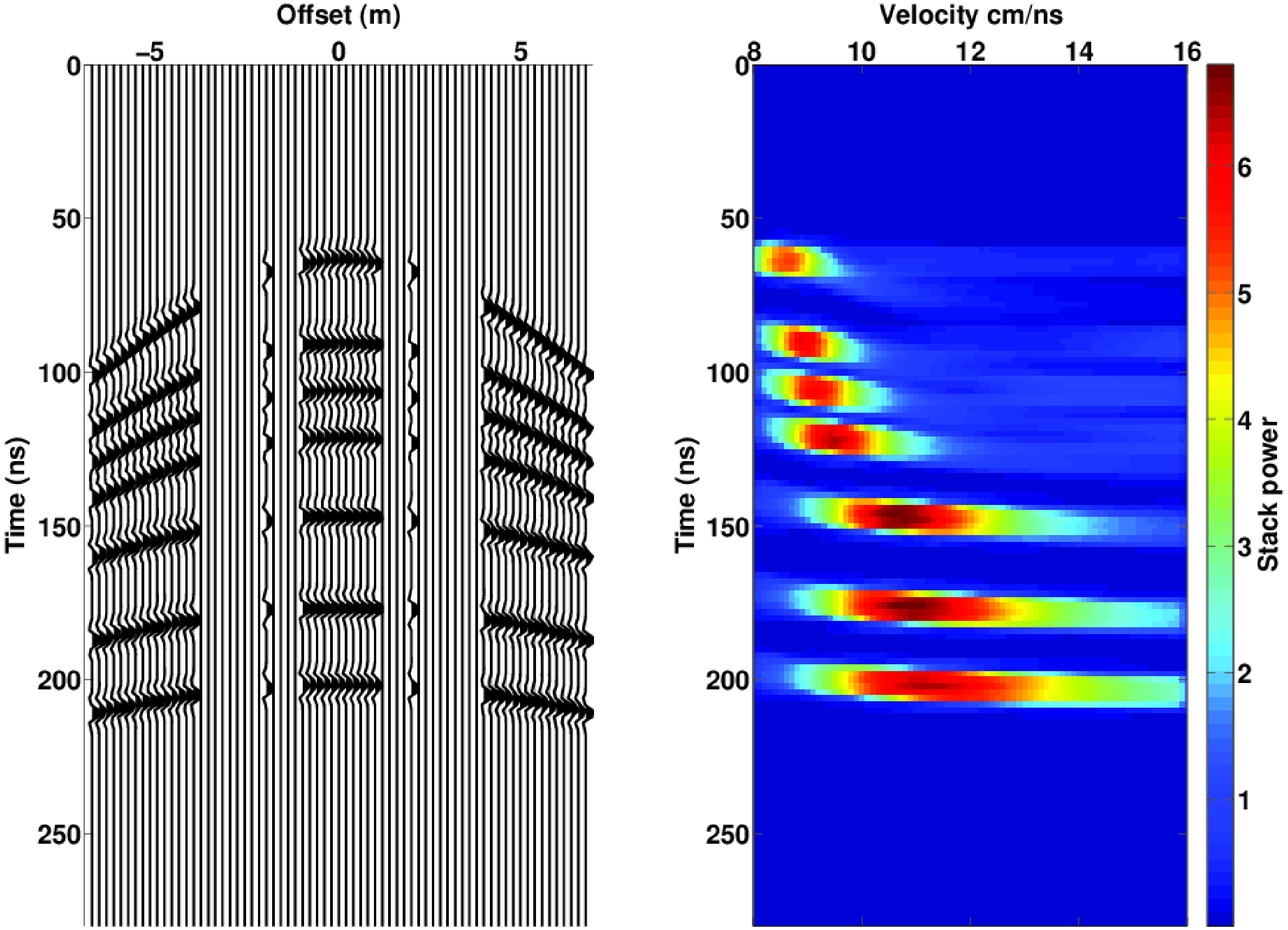

- Improved velocity resolution

Stacked section: 3.8m setup (added random noise, S/R = 1)

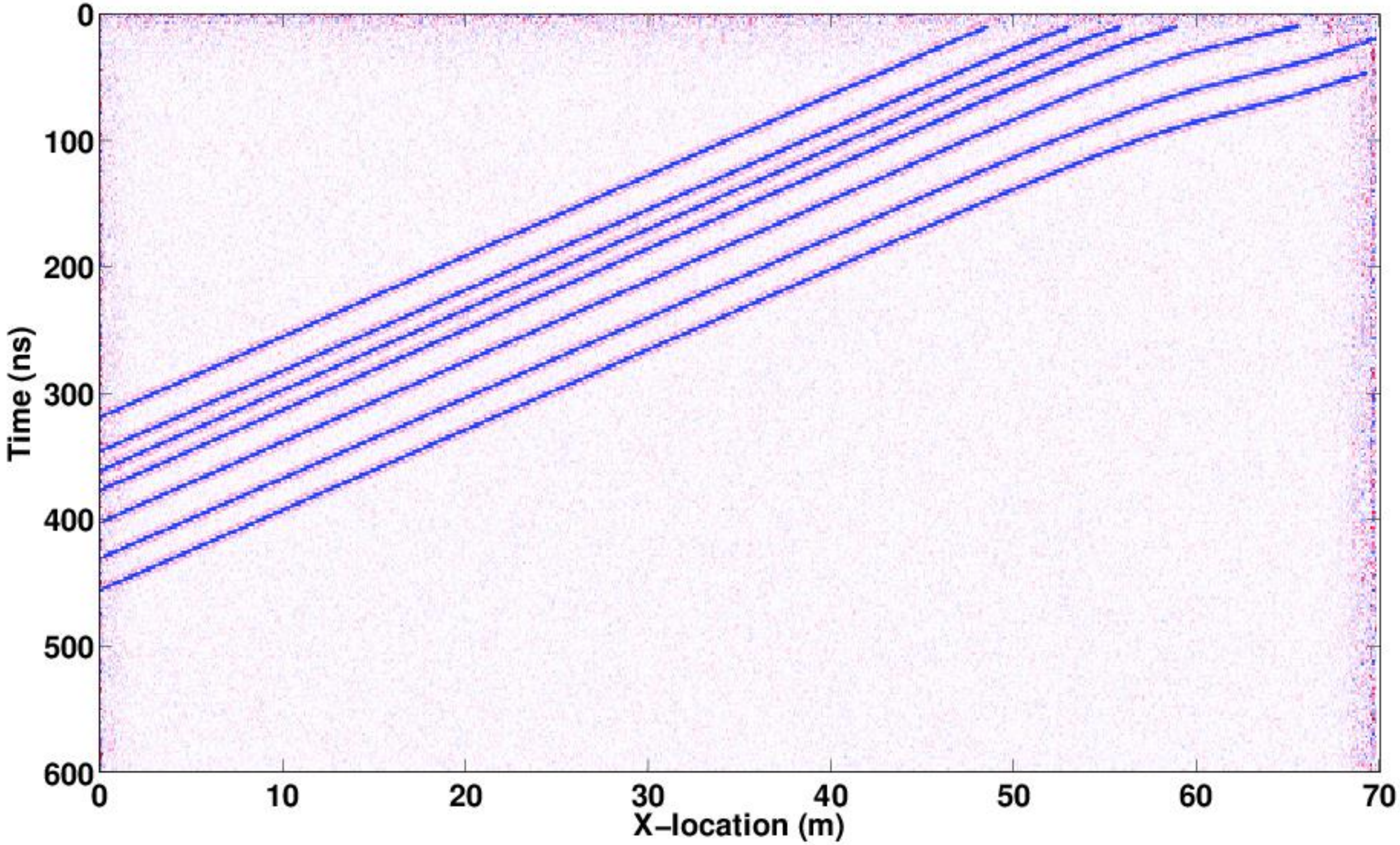

Stacked section: 6.8m setup (added random noise, S/R = 1)

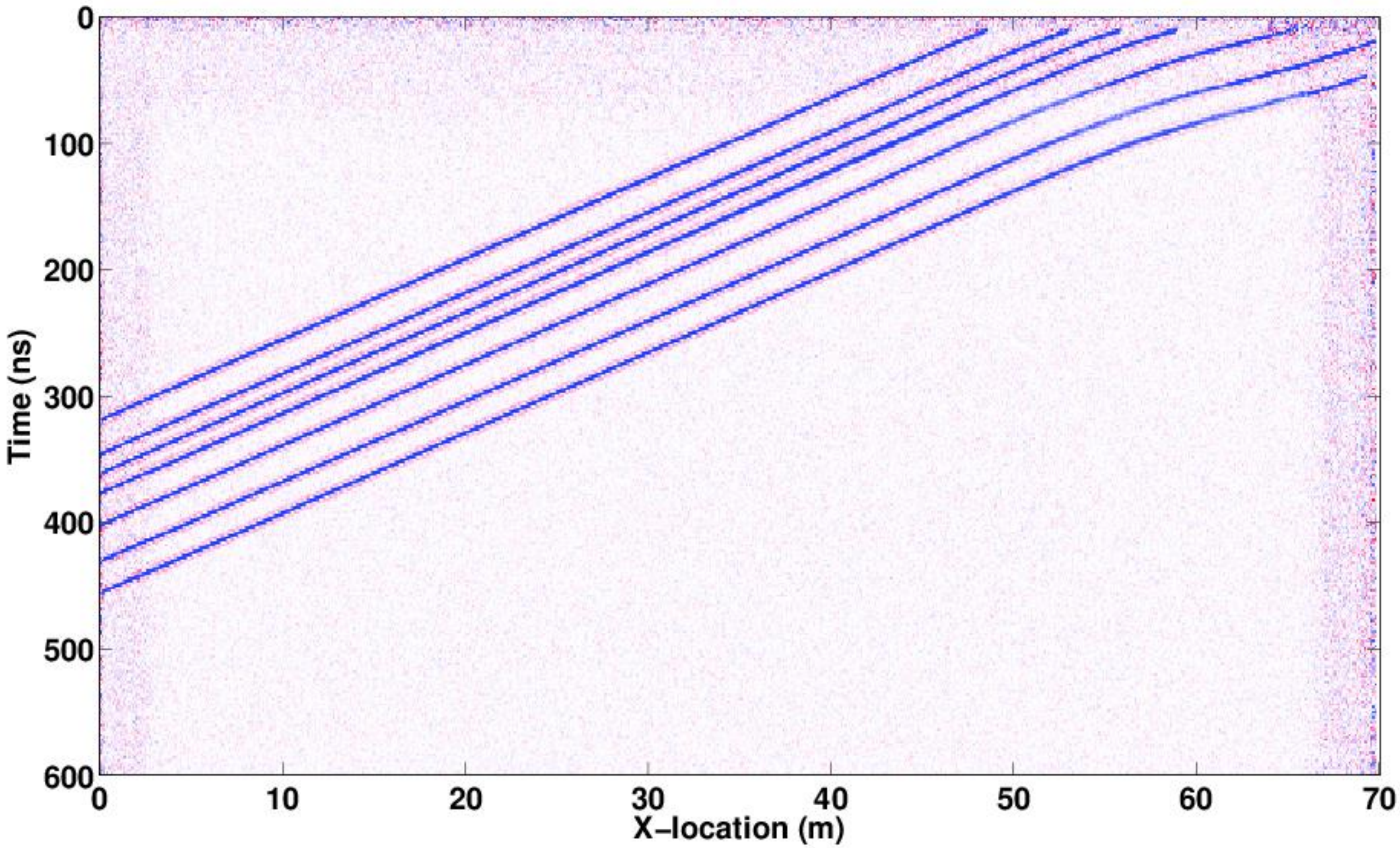

Kirchhoff time migration: 3.8m setup

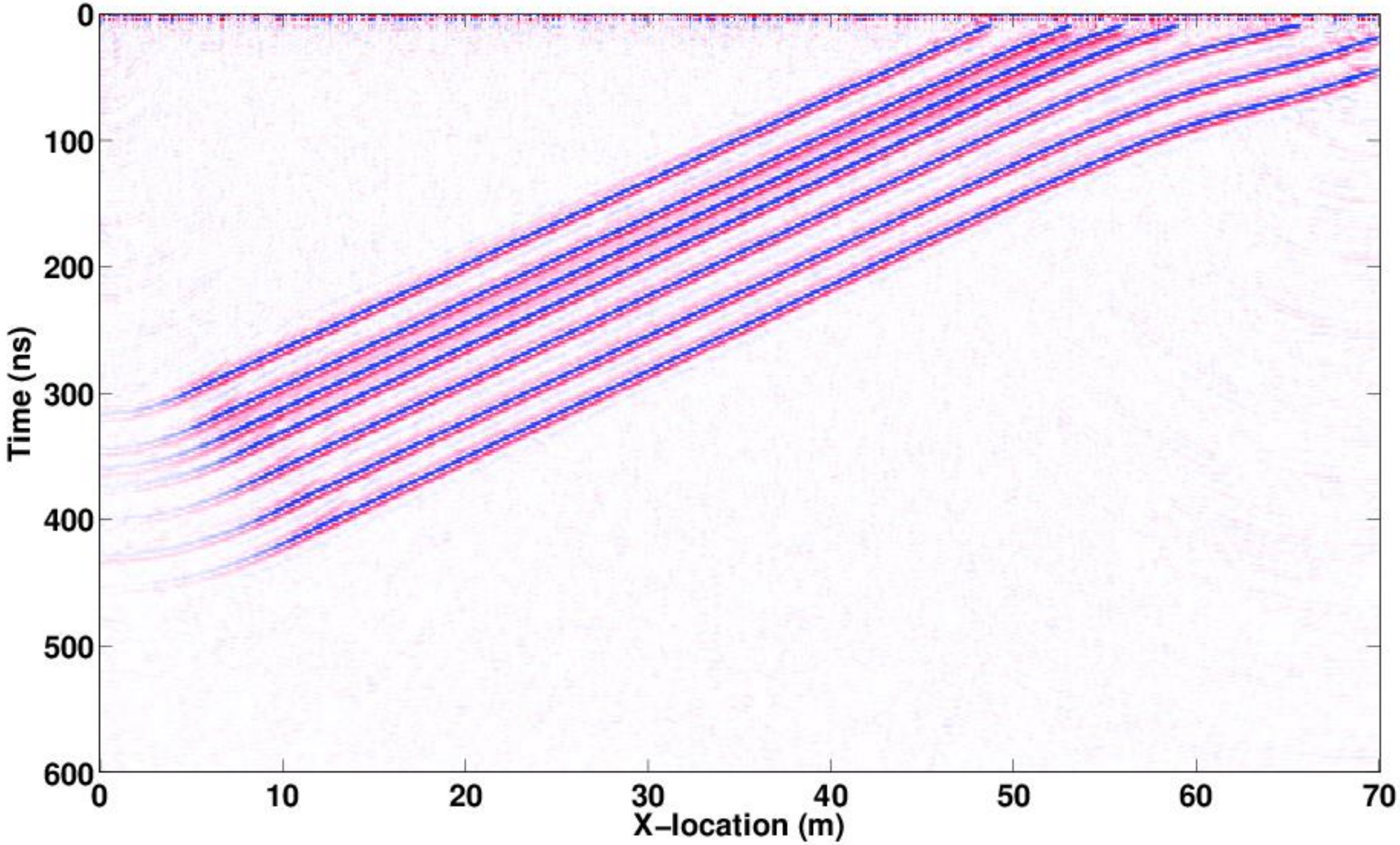

Kirchhoff time migration: 6.8m setup

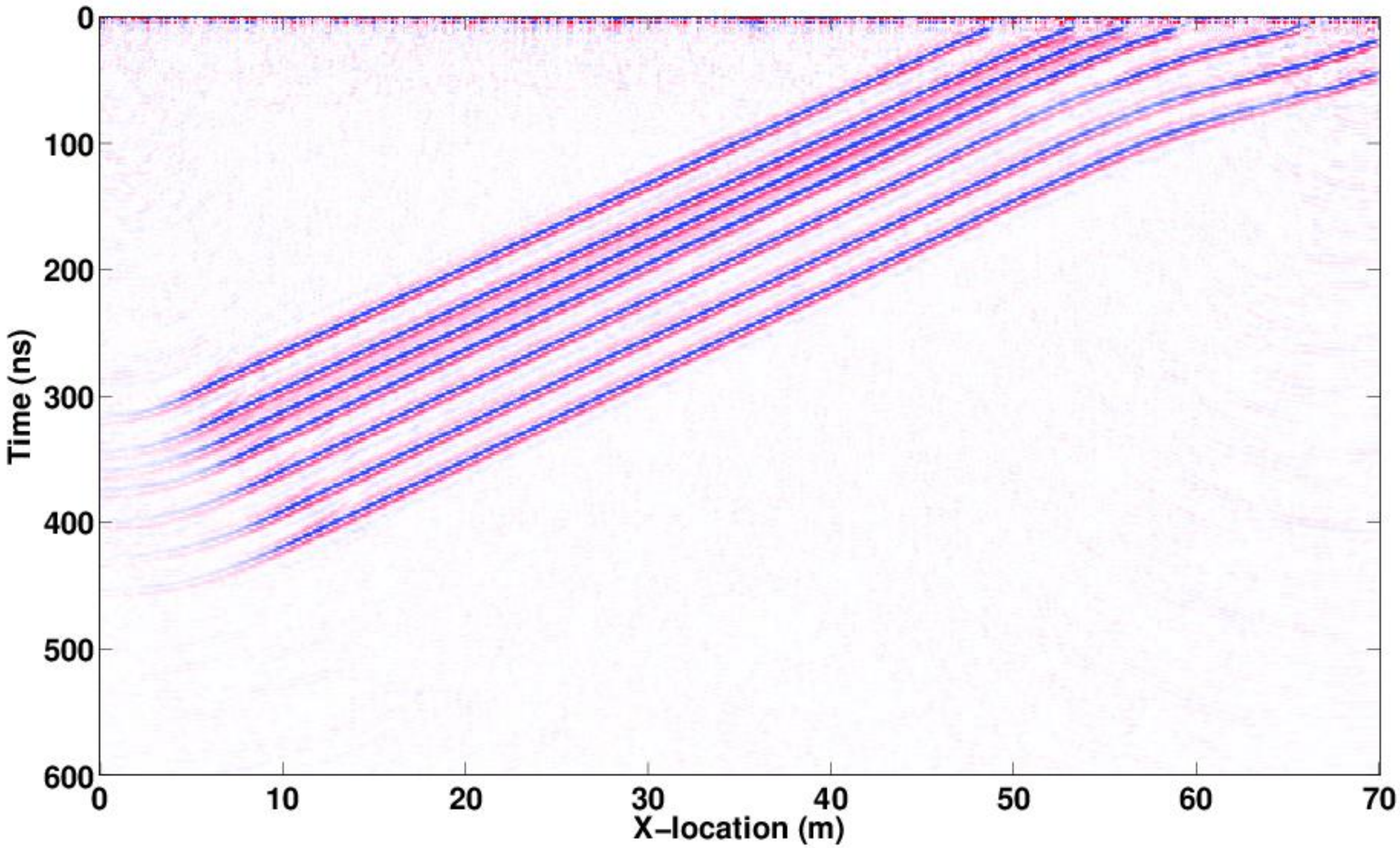

Conclusions

- Extending the separation between the two carts carrying the antennas provides larger offsets at the expense of an irregular offset sampling.

- By doubling the distance between the antennas and the cart, a maximum offset of 7.6m is possible. This configuration would provide a regular offset sampling in increments of 0.4m instead of the 0.2m given by the original design.

- Depth imaging should be considered for dealing with lateral velocity changes. Data recorded at large offsets is essential for this type of processing.

- Collecting data over a wide range of offsets will provide enough AVO (Amplitude Versus Offset) information to be used in future permitivity inversion algorithms.

Acknowledgements

- CREWES sponsors
- NSERC (Grant CRDPJ 461179-13)
- ANR (Agence Nationale de la Recherche, France)
- NORSAR
- CREWES faculty, staff and students.

Thanks!!!